Oxidation Behavior of Fe- and Ni-base Alloys in Supercritical CO_2 and Related Environments

Gordon R. Holcomb
Materials Research Engineer
National Energy Technology Laboratory
Albany, OR USA

Casey S. Carney
National Energy Technology Laboratory
and AECOM
Albany, OR USA

Richard P. Oleksak
National Energy Technology Laboratory
and AECOM
Albany, OR USA

Joseph H. Tylczak
Materials Research Engineer
National Energy Technology Laboratory
Albany, OR USA

Ömer N. Doğan
Materials Research Engineer
National Energy Technology Laboratory
Albany, OR USA

Gordon Holcomb is a Materials Research Engineer in the Structural Materials Team in the Research & Innovation Center at NETL. He received his Ph.D. from the Ohio State University in Metallurgical Engineering in 1988. Current projects cover corrosion issues in fossil energy systems. He is the U.S. Lead for the Corrosion in Supercritical Fluids task in the US-UK Collaboration on Fossil Energy Research and Development, Advanced Materials Technology Area.

Casey Carney received his B.S. in chemistry and engineering physics from Hope College. He received his Ph.D. in Chemical Engineering from the University of Colorado in 2005. He is currently an employee of AECOM as a contractor to the United States Department of Energy - National Energy Technology Laboratory in Albany, OR, where he has worked since 2008. His recent research topics have included: oxy-combustion flame analysis, thermal decomposition kinetics, and materials performance in extreme combustion and supercritical CO_2 environments.

Richard Oleksak is an AECOM Research Scientist working with the Structural Materials Team at NETL. He received his Ph.D. from Oregon State University in Chemical Engineering in 2015. His current research focuses on understanding the oxidation and corrosion behavior of structural alloys for next-generation power systems.

Joseph Tylczak is a Research Metallurgist Engineer in the Structural Materials Team in the Research & Innovation Center at NETL. He received his degree in Physical Metallurgy from Washington State University in 1979. His current work includes high temperature corrosion issues with advanced fossil fueled power systems and ambient temperature corrosion of gas transmission pipelines.

Ömer Doğan is a Materials Research Engineer in the Structural Materials Team in the Research & Innovation Center at NETL. He received his Ph.D. from Case Western Reserve University in Materials Science & Engineering in 1990. Current research focuses on the evaluation and development of heat, corrosion, and wear resistant materials for applications in harsh environments.

ABSTRACT

Materials degradation issues are a concern for implementation of indirect- and direct-fired supercritical CO_2 (sCO_2) power cycles. The oxidation response of Ni-xCr model alloys and ferritic steel Grade 91 were compared in several different high temperature environments. The environments were pure CO_2 (200 bar and ambient pressure), CO_2 with H_2O, O_2, and SO_2 impurities (ambient pressure), pure H_2O at 200 bar, and ambient pressure laboratory air. The oxidation response for many of the alloys were somewhat similar in the different environments, but exceptions were found. For example, at 700-750°C the critical Cr content to maintain a protective chromia scale in model Ni-xCr alloys (where x varied from 5 to 24 wt%) was much lower in pure CO_2 than in water containing environments or in air (<5% Cr compared to 12-14% Cr). This indicated that Ni-base superalloys may be robust in pure CO_2 environments with respect to scale spallation events or foreign object damage. Another difference was observed with respect to surface finish for Grade 91 at 550°C in CO_2 (200 bar and ambient pressure) and in laboratory air. Machined surfaces, with more cold work, resulted in the lowest oxidation rates in each environment. This indicated that surface enhancements to induce more residual stress, such as shot peening, may be of benefit for 9-12Cr ferritic-martensitic steels in sCO_2.

INTRODUCTION

Heat engine power cycles, using a working fluid of supercritical carbon dioxide (sCO_2), have the potential for high thermodynamic efficiencies when configured as a (indirect) recompression Brayton cycle [1]. Direct cycles, where pressurized oxy-combustion flue gas is utilized as the working fluid in an open loop, are also in development [2]. These sCO_2 cycles are projected to have higher efficiencies compared to steam cycles due to lack of phase change in the working fluid within the working envelope, recompression of sCO_2 near liquid densities, and high heat recuperation. In addition to lowering the environmental impact due to the higher efficiencies, dry or reduced water cooling in direct and indirect cycles, and production of storage ready CO_2 in direct cycles, will also lower the environmental impact. Furthermore, compact turbo machinery and simple configurations of the sCO_2 cycles could result in lower capital cost.

In this communication, two aspects of the oxidation behavior of alloys were compared between several indirect- and direct-cycle related environments. The first was to examine the critical Cr content needed in Ni alloys to achieve a compact and protective chromia scale. A series of Ni-xCr model alloys were made and used for these tests. The second was to examine the effect of surface finish on the oxidation behavior of Grade 91 ferritic-martensitic steel.

EXPERIMENTAL PROCEDURES

A series of model alloys were produced using commercial-type techniques to obtain Ni-xCr alloys where the microstructures and impurity levels were similar to commercial alloys. First, a binary master alloy of NiCr was made from commercial purity feed stocks using vacuum induction melting (VIM) followed by electro-slag reduction (ESR) to reduce O and S levels [3,4]. The ESR slag was 40% CaF_2 -30% CaO - 30% Al_2O_3 (wt%), and the master alloy ingot was approximately 80 kg. Final alloys were made with VIM combining the master alloys with Ni (or sometimes hot top material from a previous melt). Computationally optimized homogenization heat treatments [5] were done, then the ingots were machined to remove surface defects. Wrought processing involved wrapping the ingots in stainless steel foil and preheating for 3 h prior to upset forging and forged flattening. Each ingot was step forged and squared in multiple operations to 3.2 cm, then hot rolled to approximately 0.25 cm.

The Grade 91 alloy was machined from seamless tubing (5.7 cm outside diameter), manufactured by Vallourec & Mannesmann Tubes, which had undergone normalizing at 1060 °C for 20 min and tempered at 780 °C for 60 min.

Compositions of each alloy are given in Table 1.

Table 1. Alloy compositions. Grade 91 values are from the manufacturer. Model alloy values are from wavelength dispersive x-ray fluorescence spectroscopy using a Rigaku ZSX Primus II, except for the interstitial elements that are from combustion (C and S using a Leco CS744) and inert gas fusion (O and N using a Leco ON736) methods.

Alloy	Ni wt%	Cr wt%	Al wt%	Si wt%	Mn wt%	Co wt%	Ti wt%	Fe wt%	Cu wt%	C ppm	N ppm	O ppm	S ppm
91	0.14	8.46	0.01	.036	0.44			Bal	0.16	1000	545		20
Ni5Cr	Bal	5.00	0.02	<0.01	0.02	0.03	0.01	<0.01	0.01	38	8	6	3
Ni12Cr	Bal	12.08	0.01	<0.01	0.01	0.12	<0.01	<0.01	<0.01	233	26	62	13
Ni14Cr	Bal	14.09	0.02	<0.01	<0.01	0.14	<0.01	<0.01	<0.01	311	29	15	7
Ni16Cr	Bal	16.04	0.02	<0.01	<0.01	0.22	0.01	0.02	<0.01	226	43	65	15
Ni18Cr	Bal	18.13	0.04	<0.01	<0.01	0.25	<0.01	0.02	0.01	270	50	17	8
Ni20Cr	Bal	20.08	0.03	<0.01	<0.01	0.26	<0.01	0.05	0.01	228	72	44	12
Ni22Cr	Bal	22.10	0.05	<0.01	<0.01	0.39	<0.01	0.16	<0.01	149	88	27	12
Ni24Cr	Bal	24.06	0.03	<0.01	<0.01	0.31	<0.01	0.12	0.01	119	96	38	16

Samples were machined from each alloy that were 19 × 13 × 2 mm in dimension, with a 5-mm hole near the top middle of the coupon for hanging the sample during exposure. The model nickel alloy coupons were surface finished first by lapping with 17.5 µm alumina, then with a final finish using 600 grit SiC paper. The coupons were dimensioned, ultrasonicated in isopropyl alcohol, and weighed.

The Grade 91 coupons were surface finished three ways. One was a “standard” (or 91S) preparation and was prepared as the model nickel alloys. Another was a preparation that retained more “cold work” (or 91CW). In these samples, no lapping or 600 grit paper steps were used—for as-machined surfaces. The last surface preparation retained the least cold work and was done by lapping followed by a single 2-hour polishing step using “colloidal silica” (or 91CS) until a mirror finish was achieved.

The alloys were exposed in six environments: sCO_2, atmospheric pressure CO_2 (aCO_2) [6], two direct-cycle type environments DF4 and DF4S, supercritical H_2O (sH_2O) [6,7], and laboratory air [8]. The sCO_2 exposures were in a flowing CO_2 autoclave constructed from Haynes 230. The autoclave was purged 10 times with Ar by cycles of 1 to 7 to 1 bar, and then heated to 700 °C. Research grade CO_2 was then introduced at ~10 g/min. Once the target pressure was reached, the CO_2 flow was reduced to 2 g/min. The DF4 and DF4S exposures were done in horizontal tube furnaces. Mass flow meters were used to introduce CO_2, O_2 and SO_2 (mixed prior to entry into the furnace); a syringe pump was used to drip water into a pan within the furnace to flash to steam. Test durations were nominally 500 h, after which the samples were weighed and put back into a subsequent test. Table 2 summarizes the test environments.

Table 2. Test types and environments.

Test	Gas composition	Gas Notes	Alloys	T, °C	P, bar	Flow rate at T/P, cm/min
sCO_2	CO_2	99.999% CO_2	Ni-xCr	700	200	0.8
			91	550	200	0.7
aCO_2	CO_2	99.999% CO_2	Ni-xCr	700	1	25
			91	550	1	25
DF4	CO_2+4%H_2O+1%O_2	Deionized H_2O	Ni-xCr	750	1	25
DF4S	CO_2+4%H_2O+1%O_2+0.1 %SO_2	Deionized H_2O	Ni-xCr	750	1	25
sH_2O	H_2O	Deaerated deionized H_2O	Ni-xCr	700	200	2
Air	Laboratory air	Some H_2O present from relative humidity	Ni-xCr	700	1	0
			91	550	1	0

The exposed coupons were weighed using a balance capable of measuring 10-5 grams to determine the mass change. A scanning electron microscope (FEI Inspect) with energy dispersive spectroscopy (EDS) capabilities was used to obtain images and microchemical data on the exposed surfaces and cross-sections.

RESULTS AND DISCUSSION

Nickel-Chromium Model Alloys

Mass loss changes with time are shown in Fig. 1 for the Ni-xCr model alloys. In sCO_2, all of the mass changes were small, but those for Ni-5Cr were markedly higher than for the higher Cr alloys. In aCO_2, the mass changes were higher than in sCO_2, but still low. In contrast with sCO_2, Ni-5Cr had the smallest mass change in aCO_2. This was the only environment where this occurred. There was no pattern, with respect to Cr levels, in the mass change data for 12-24 Cr alloys in the pure CO_2 environments. In sH_2O there was a distinct trend with Cr, with mass change in 5Cr > 12Cr > 14Cr > 16-24Cr. The high mass gain for Ni-5Cr in sH_2O clearly indicates that a protective chromia layer was not established and maintained. The mass gains for the DF4 and DF4S environments were similar. In both cases Ni-5Cr had high mass gains and the remaining alloys had quite low mass gains. The mass gains in DF4S were somewhat higher than in DF4—showing an effect with 0.1% SO_2. The results in air (for significantly longer exposures than the other environments) also had quite high mass gains for Ni-5Cr. When Ni-5Cr is removed from the chart (lower right in Fig. 1), the results show low mass gains followed by mass losses. This could be a result of spalling or chromia evaporation. The laboratory air used had some water from the relative humidity in the room, which would favor reactive evaporation of chromia as CrO2(OH)2(g) [9].

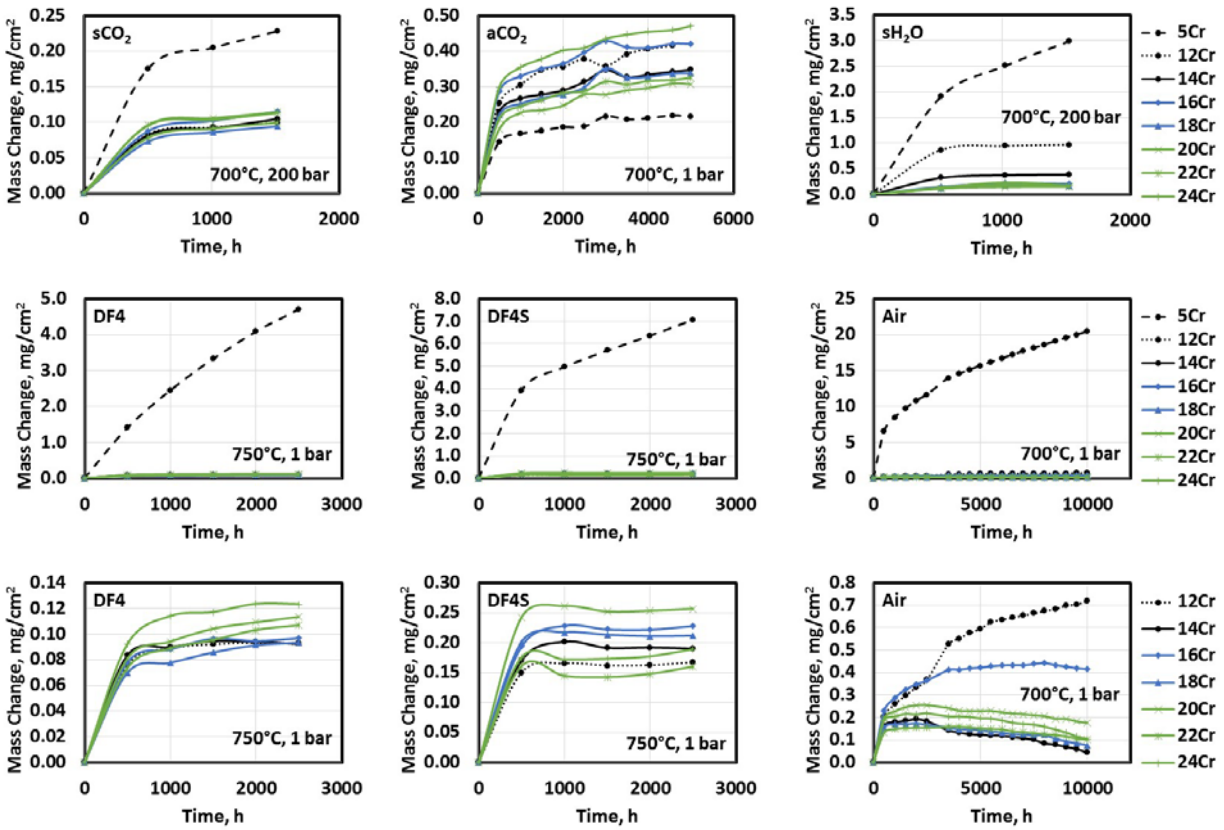

Fig. 1. Mass change results as a function of time for Ni-xCr model alloys in six environments. The bottom row repeats the middle row, but without the heavily oxidized Ni-5Cr data.

Mass change data after 1500 h are shown in Fig. 2 as a function of Cr for the six environments. There are clear differences in the critical Cr level needed to form and maintain a protective chromia scale. The Ni-5Cr alloy in the pure CO_2 environments (sCO_2 and aCO_2) was protective, while it wasn't in the other environments. When H_2O or O_2 was part of the gas phase, a transition to protective kinetics occurred somewhere between 5-12Cr in DF4, DF4S and air, and at 14Cr in sH_2O. The oxygen activity in sCO_2 and sH_2O are similar (1.8×10^{-6} and 2.2×10^{-6} atm, respectively at 700°C and 200 bar), so it is the H_2O itself that is more aggressive than CO_2 for the Ni-5Cr alloy.

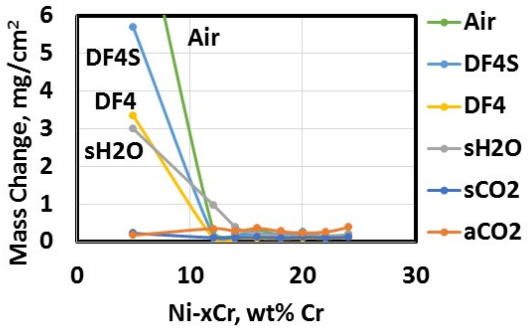

Fig. 2. Mass change results after 1500 h for Ni-xCr model alloys in 6 environments.

Figure 3 shows cross section microstructures after 2000 h of exposure in aCO_2 at 700 °C. The oxide scale for Ni-5Cr shows a duplex oxide scale. Elemental analysis with EDS showed that the inner oxide scale

was Cr oxide (likely Cr_2O_3) with Ni also present, while the outer oxide scale was Ni oxide (presumably NiO). The microstructure for Ni-12Cr showed a sharp transition between an inner and outer oxides, but both were essentially pure Cr oxide (Cr_2O_3). The microstructures for Ni-14Cr and Ni-24Cr both showed contrast between inner and outer layers of Cr oxide (Cr_2O_3), but without the sharp transition seen with Ni-12Cr.

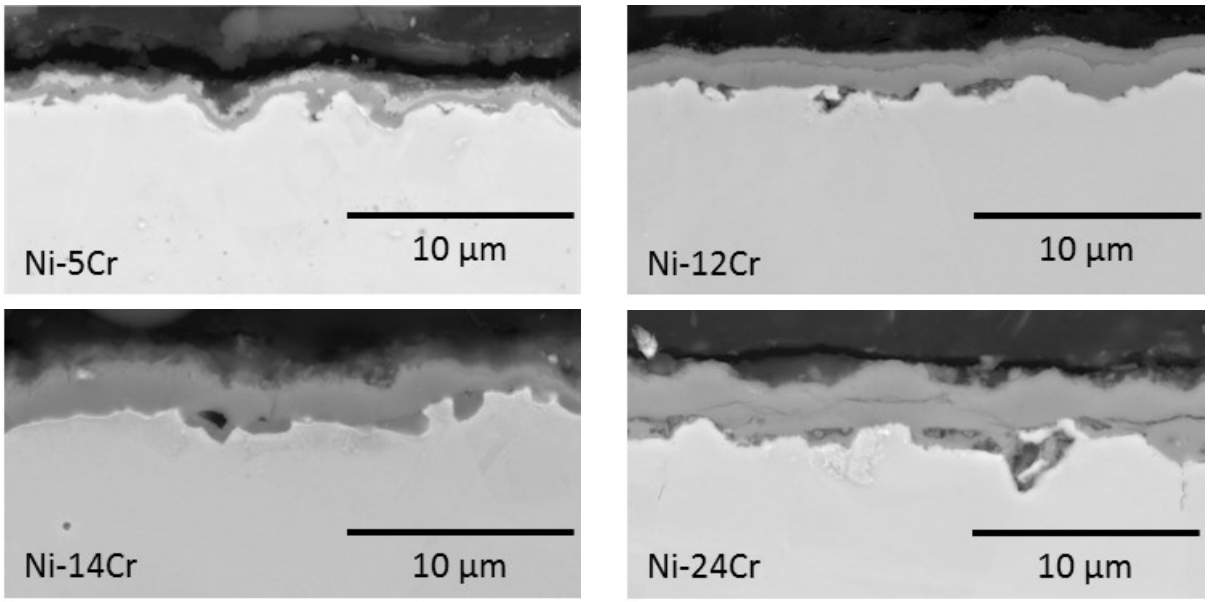

Fig. 3. Ni-xCr alloys after 2000 h exposure in aCO_2 at 700 °C. The images are backscattered SEM.

The oxide scale for Ni-5Cr was thinner than the other three compositions shown in Fig. 3, which corresponds to the results shown in Fig. 1 for aCO_2. It is likely that some amount of NiO spalled during heating, cooling, or post-test handling, which lowered the mass change curve in Fig. 1 to lower values than the other (higher Cr) alloys.

Figure 4 shows cross section microstructures after 2000 h of exposure in air at 700 °C. The oxide scale for Ni-5Cr is much thicker than the other compositions in Fig. 4. Elemental analysis with EDS showed a clear and sharp transition between an inner scale of Cr-Ni oxide (likely a spinel) and an outer scale of Ni oxide (NiO). The cross-sections of the other three compositions in Fig. 4 were much thinner and were primarily Cr oxide (Cr2O3). The cross-sections were after 2000 h, which was prior to the mass decreases seen in Fig. 1 in air for Cr compositions of 12 and higher.

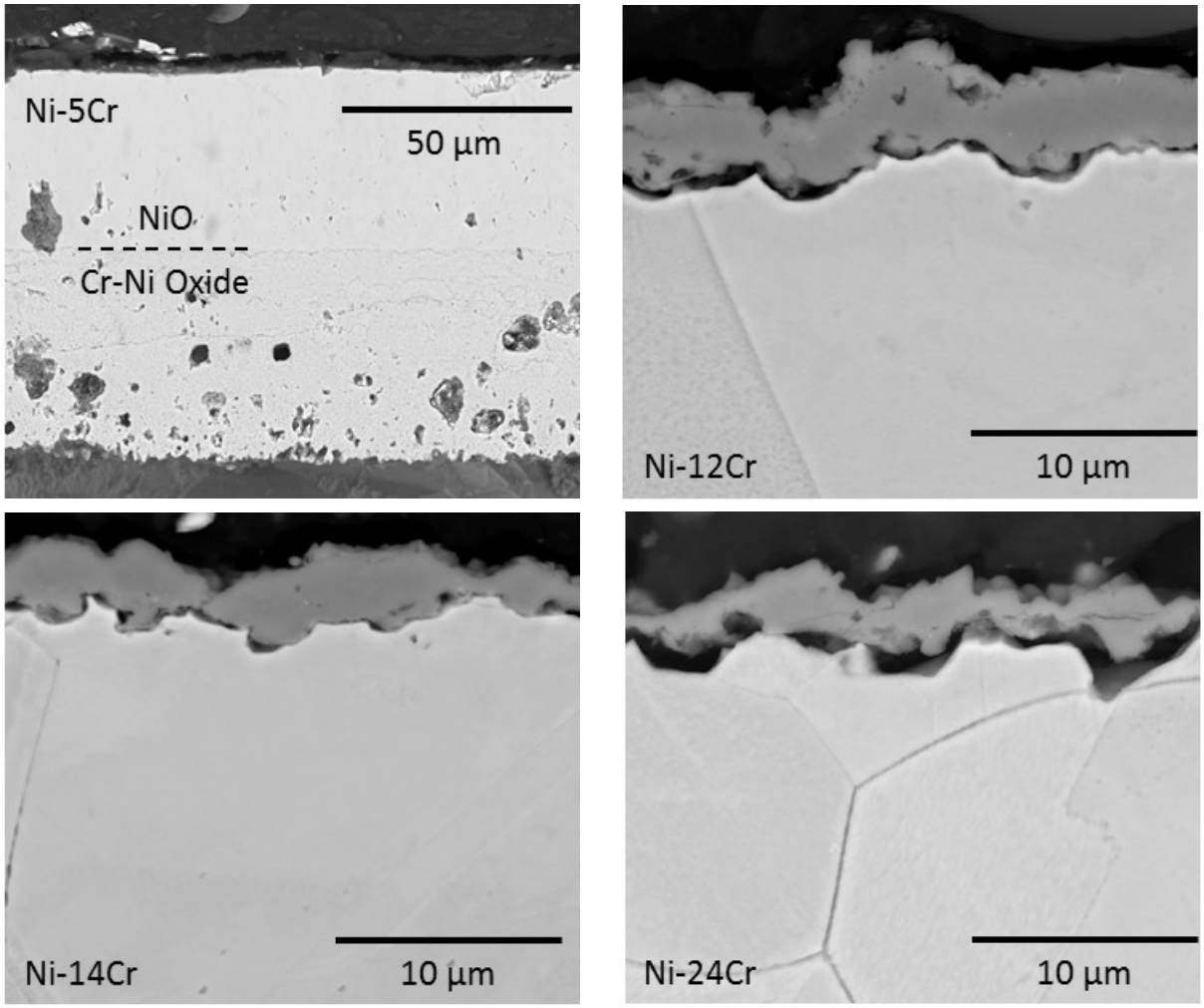

Fig. 4. Ni-xCr alloys after 2000 h exposure in laboratory air at 700 °C. The images are backscattered SEM.

Figure 5 shows a cross-section and elemental maps of Ni-12Cr after 2000 h at 700C for a portion of the cross-section with an unusual feature. The feature is a pit-shaped depression, filled with Cr-oxide (Cr_2O_3), underneath an outer oxide dome of Ni-oxide (NiO). One explanation for the structure is that a chromia scale did not initially form at that location. A less protective scale of NiO formed, which resulted in the pit. A chromia scale eventually did form at the metal-scale interface. As the chromia layer grew, it pushed out the NiO scale; it is the remnant of the initial NiO scale that is now seen at the outer oxide location.

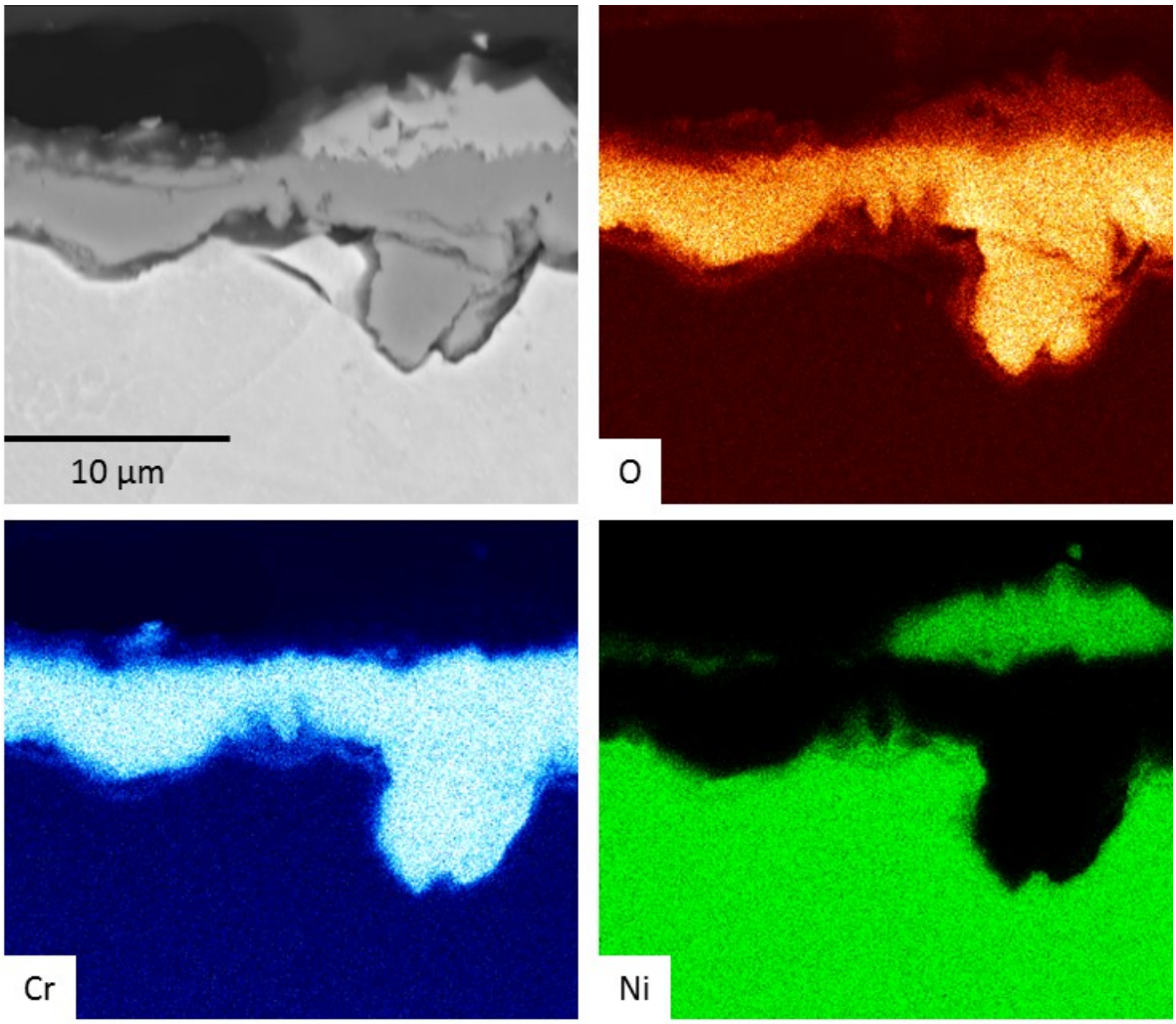

Fig. 5. Ni-12Cr after 2000 h exposure in laboratory air at 700 °C showing backscattered SEM and EDS elemental maps.

Although it should be further verified, the results of exposures of Ni-xCr alloys in sCO_2 (indirect cycle) and DF4/DF4S (direct cycle) environments indicate that the high strength Ni-base superalloys (generally 19-25%Cr) may be quite resilient to recovery from foreign object damage. Under normal use, Cr is depleted under the protective chromia scale that forms. If the scale is breeched (such as from an impact), then the newly exposed alloy will have a lower Cr level than the original alloy. The ability to regenerate a new protective chromia scale down to 12%Cr in pure CO_2, DF4, and DF4S, and to provide some protection down to 5% Cr pure CO_2, should make these superalloys resilient. However, it remains to be seen if the other alloying elements in these superalloys interfere with this low Cr protectiveness.

Surface Finish Effects in Grade 91steel

It is well-known that shot peening, and similar surface preparations, can greatly reduce scaling in ferritic steel tubing and piping in steam boilers. Shot peening adds cold work to the near surface of the alloy, which can increase the diffusion of Cr to the surface during oxidation, decreasing the rate of oxidation. In this study, cold work effects were examined for grade 91 steel exposed to aCO_2 and sCO_2. For comparison, the alloy was also exposed to air. In this study, machining added cold work to the surface. Figure 6a shows the machined surface. The 91CW samples have more near-surface cold work than the other 2 conditions. After machining, a lapping step was done (Fig. 6b). Then either 600 grit paper (91S, Fig. 6c) or a colloidal silica polish (91CS, Fig. 6d) was done. The colloidal silica polish was aimed at removing the lapped

damage, without adding cold work (which the 600 grit paper adds). The 91CS samples had the least cold work. Fig. 6d shows that despite the samples appearing highly reflective at this stage, not all of the lapping damage was removed by the colloidal silica process—some surface voids remain.

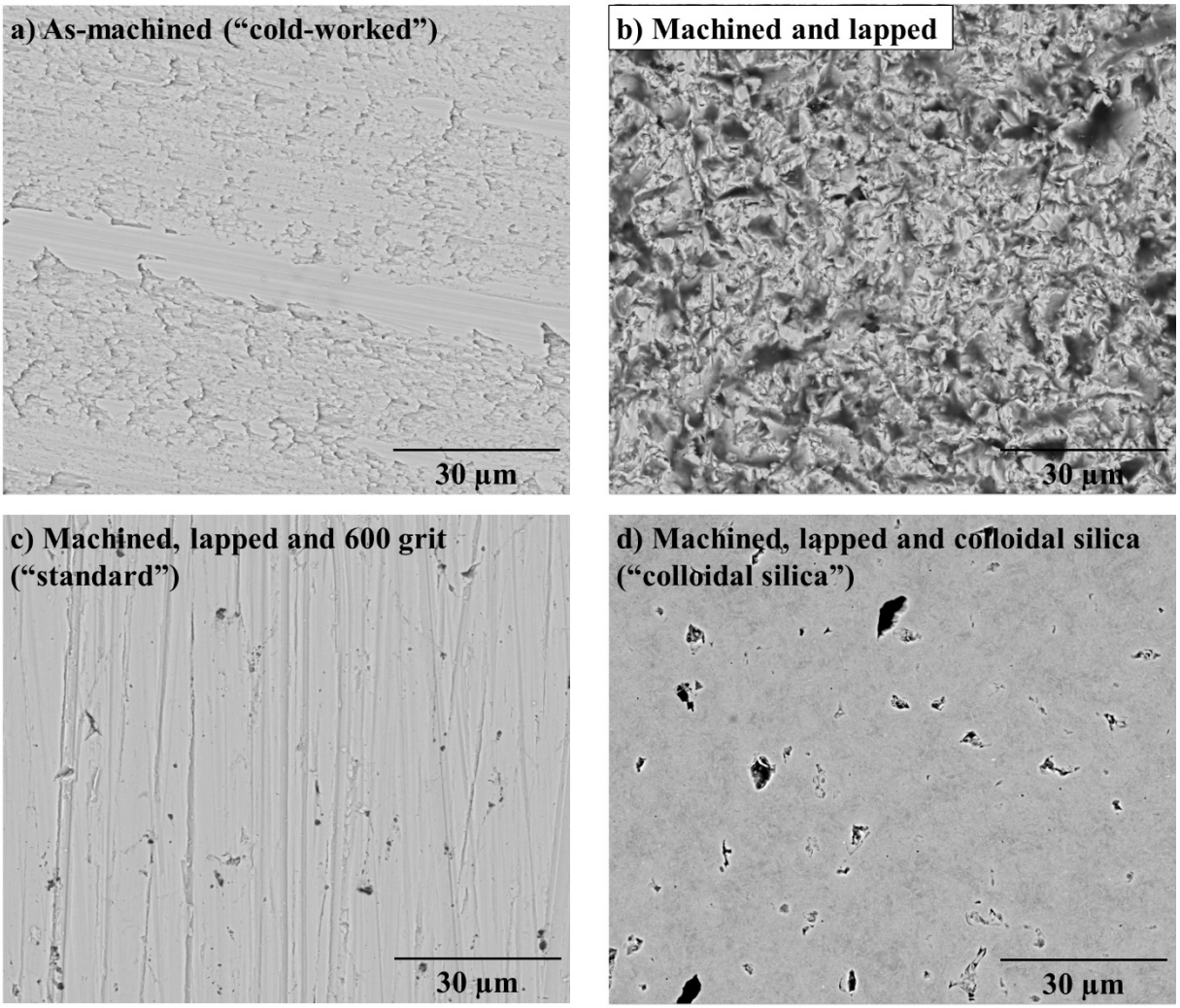

Figure 6. Backscattered SEM surface images of alloy 91 with four different surface finishes. (a), (c), and (d) show the surfaces of samples 91CW, 91S, and 91CS, respectively.

Mass change results are shown in Fig. 7 after exposures in sCO_2, aCO_2, and air. The mass gains in air were much lower than in the CO_2 environments. There were distinct differences in the surface finish effect in the three environments. The 91CW samples had the least mass gains in each environment. In sCO_2 and air, the 91S and 91CS samples were similar (in their respective environment). However, in aCO_2, the 91CS samples had mass gains like 91CW. The 91S results were similar to those found by Rouillard [10] with similar surface preparation after 550 °C/1 bar and 550 °C/250 bar exposures.

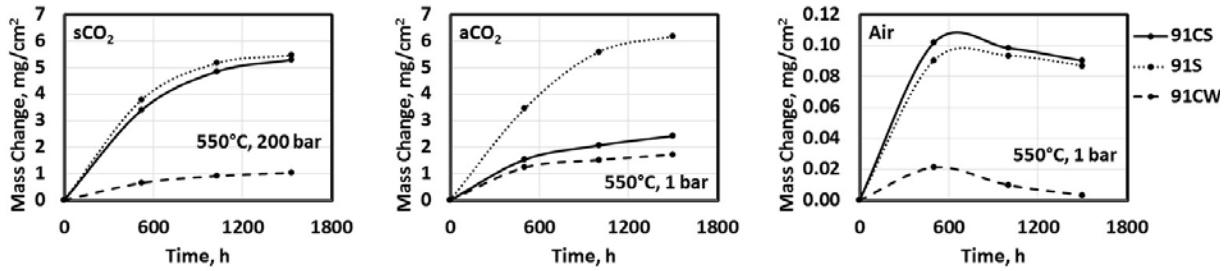

Fig. 7. Mass change results as a function of time for alloy 91 with different surface finishes in 3 environments.

The benefits of cold work are clear. However, in the CO_2 environments, the mass changes are still high compared to those found in alloys such as 600, 690, and 800 with mass gains on the order of 0.02 mg/cm^2 after 1000 h at 550 °C/100 bar [11]. These are chromia forming alloys whereas Grade 91 forms a thicker duplex scale with an inner Fe-Cr spinel layer and an outer magnetite layer [10]. Such thick scales are not desirable in heat exchanger components, but may be adequate for piping applications.

SUMMARY

The oxidation responses of Ni-xCr model alloys (where x varied from 5 to 24 wt%) were compared in six high temperature environments. The Ni-5Cr alloy in pure CO_2 environments (sCO_2 and aCO_2) was at least somewhat protective, while it was unprotective in the other environments. When H_2O or O_2 was part of the gas phase, a transition to protective kinetics occurred somewhere between 5-12Cr in DF4, DF4S and air, and at 14Cr in sH_2O. The oxygen activity in sCO_2 and sH_2O were similar, so H_2O was more aggressive than CO_2 for the Ni-5Cr alloy. The ability to remain protective at low Cr values indicates that nickel base superalloys may be resilient to damage that exposes near-surface alloy that is depleted Cr—especially in pure CO_2.

The oxidation responses of ferritic steel Grade 91, with three different surface finishes, were compared in three different environments at 550 °C. The mass gains in air were much lower than in CO_2 environments. The benefits of near surface cold work were observed—the samples with the most cold work had the smallest mass gains in all three environments. This indicates that surface enhancements to induce more residual stress, such as shot peening, may be of benefit for 9-12Cr ferritic-martensitic steels in sCO_2.

ACKNOWLEDGEMENTS

This work was performed in support of the US Department of Energy's Fossil Energy Crosscutting Technology Research Program. The Research was executed through NETL Research and Innovation Center's Advanced Alloy Development Field Work Proposal. Research performed by AECOM Staff was conducted under the RES contract DE-FE-0004000.

REFERENCES

[1] R.A. Dennis, “U.S. DOE R&D Program on Supercritical CO_2 Power Cycles,” in Proceedings: EPRI International Conference on Corrosion in Power Plants, EPRI-3002006972, Palo Alto, CA, 2015, 3002006972, pp. 2-136 to 2-153.

[2] R.J. Allam, “NET Power's CO_2 cycle: the breakthrough that CCS needs,” in Modern Power Systems, http://www.modernpowersystems.com/features/featurenet-powers-co2-cycle-the-breakthrough-that-ccs-needs/, 2013.

[3] P. D. Jablonski and J. A. Hawk, “Nitrogen Control in VIM Melts,” in the Proceedings of the 2013 International Symposium on Liquid Metal Processing & Casting, Eds. M. J. M. Krane, A. Jardy, R. L. Williamson, and J. J. Beaman, TMS, 2013, pp. 315-319.

[4] P. D. Jablonski and J. A. Hawk, “The Practical Application of Minor Element Control in Small Scale Melts,” in the Proceedings of the 2013 International Symposium on Liquid Metal Processing & Casting, Eds. M. J. M. Krane, A. Jardy, R. L. Williamson, and J. J. Beaman, TMS, 2013, pp. 329-332.

[5] P. D. Jablonski and J. A. Hawk, Journal of Materials Engineering and Performance, 26, 1(2017): pp. 4-13.

[6] G. R. Holcomb, Ö. N. Doğan, C. Carney, “Oxidation of Alloys for Energy Applications in Supercritical CO_2 and H_2O,” Corrosion Science, 109 (2016): pp. 22-35.

[7] G. R. Holcomb, “High Pressure Steam Oxidation of Alloys for Advanced Ultra-Supercritical Conditions,” Oxidation of Metals, 82, 3-4(2014): pp. 271-295.

[8] G. R. Holcomb, J. Tylczak, and C. Carney, “Oxidation of CoCrFeMnNi High Entropy Alloys,” JOM, 67, 10(2015): pp. 2326-2339.

[9] G. R. Holcomb, “Steam Oxidation and Chromia Evaporation in Ultra-Supercritical Steam Boilers and Turbines,” Journal of the Electrochemical Society, 156, 9(2009): C292-C297.

[10] F. Rouillard, G. Moine, L. Martinelli, and J. C. Ruiz, “Corrosion of 9Cr Steel in CO_2 at Intermediate Temperature I: Mechanism of Void-Induced Duplex Oxide Formation,” Oxidation of Metals, 77, 1-2(2012): pp. 27-55.

[11] H. J. Lee, G. O. Subramanian, S. H. Kim, and C. Jang, “Effect of pressure on the corrosion and carburization behavior of chromia-forming heat-resistant alloys in high-temperature carbon dioxide environments,” Corrosion Science, 111 (2016): pp. 649-658.